ARTICLE

Mechanical Performance and Stamping Formability of Ti/Al Multilayer Composites Under Interface Constraint Effect

Cao Miao[1], Deng Kunkun[2], Chen Huiqin[1], Duan Xingwang[1], Xu Yue[1], Li Fei[1], Che Xin[1], Wang Zhenbo[1], Yang Jingran[1], Zhang Zhihao[1], Li Ye[1]

[1] College of Materials Science and Engineering, Taiyuan University of Science and Technology, Taiyuan 030024, China; [2] College of Materials Science and Engineering, Taiyuan University of Technology, Taiyuan 030600, China

Abstract: Ti/Al layered metal composites (LMCs) with 3, 5 and 7 layers were prepared via hot-pressing followed by hot-rolling at 500 °C. The crack initiation and growth behavior in LMCs during tensile and Erichsen cupping tests were explored. The influence mechanism of interface constraint on the mechanical performance and stamping formability of LMCs was analyzed. Results show that LMCs exhibit strong interfacial bonding due to intermetallic phase with micron-scale thickness. As the layers of LMCs increase, their yield strength (YS) and ultimate tensile strength (UTS) increase accompanied with the reduction in the elongation (EL) and toughness, and their anisotropy of mechanical performance increases obviously due to the strong basal texture formed by hot-rolling. Meanwhile, both the work-hardening exponent (n) and plastic strain ratio (r) decrease, but the yield strength ratio (σ_s/σ_b) increases, which deteriorates the stamping formability of LMCs. Interfacial delamination plays a crucial role in the fracture for LMCs with fewer layers. The interface is prone to delamination because of poor interfacial bonding, which delays the fracture failure of LMCs by inhibiting crack initiation, promoting crack deflection and passivation, and reducing the driving force of crack propagation.

Key words: Ti/Al multilayer composites; tensile; Erichsen cupping tests; interface

As structural materials, both lightweight Al and high-strength Ti have been developed and used in the automobile and aerospace industry[1–2]. Ti and its alloys have the advantages of high specific strength, high specific stiffness, high temperature resistance, corrosion resistance, etc, but the high price greatly restricts their commercial application. Al and its alloys also received much attention because of their abundant reserves, light weight and low price. However, Al and its alloys have poor corrosion resistance and high temperature impact performance, which restricts their application in specific fields. Therefore, it is considered that Ti and Al are combined as Ti/Al laminated composites to obtain unique properties such as high strength, high stiffness, high toughness, low cost and lightweight. In addition, due to the change of the stress state near Ti/Al interface, Ti/Al laminated composites may obtain some unexpected properties. As a consequence, Ti/Al laminated composites have captured great attention because of their excellent comprehensive performances recently[3–4]. The interface plays a vital role during the deformation of Ti/Al laminated composites. Our previous works reported that the interface can make a profound difference to the deformation mechanism of Ti/Al composites[5]. It has been proved that the interface adjusts the deformation of component metals via transferring stress/strain during deformation. Also, the interface can effectively restrict crack propagation via crack deflection, blunting, shielding, bridging, trapping, etc[6–8]. In short, the evolution of interfacial structure and performances affects the failure mechanism. Other studies also show that there is interfacial heterogeneity and interfacial promoting deformation[9]. Zhang et al[10] prepared ZW31/PMMCs composites with 2, 3, 5 and 7 interfaces, and found that the soft and hard layers exhibit more harmonious deformation for composites with more interfaces. The main crack extends to the particle reinforced metal matrix

composites (PMMCs) layer and releases energy through microcrack, which passivates the crack-tip and increases the crack growth resistance. Finally, both ultimate tensile strength (UTS) and elongation (EL) are enhanced. The effect of the number of interface (2, 4 and 8 interfaces) on the deformation behavior of Ti/Al composites was explored by Fan et al[11]. It is showed that the composites with 8 interfaces possess the greatest interfacial metallurgical bonding, which enhances the coordination deformation of each layer. Thus, Ti/Al composites with good fracture elongation, excellent flexural strength and deep drawability are obtained. In short, the change of the number of interface leads to the difference of stress-strain state in the deformation of the composites. So it is essential to study the effect of multi-interface constraint on the mechanical performance and stamping formability of layered multilayer composites (LMCs).

Recent researches on Ti/Al composites are mostly concentrated on improving the fabrication technique, exploring the interfacial evolution dynamics, etc. There are a few researches on the formability. Many structural parts manufactured by stamping forming have great application potential in various fields of production and life. Fan et al[11] preliminarily conducted punch bulging test and deep drawing test on Ti/Al composites to test their forming limit and deep drawability. Further, Kaya et al[12] explored the influence factors of forming limits of Ti/Al multilayer sheets, including strain rate, temperature and loading condition. Most researches on the stamping formability of Ti/Al composite sheet focus on the forming process and other macro aspects. In this study, the stamping forming mechanism of Ti/Al LMCs will be explored from a microcosmic perspective around the interface. Erichsen cupping test is a reliable way to evaluate the stamping formability of the sheet, which deserves further exploration[5].

In current work, Ti/Al LMCs with 3, 5 and 7 layers were designed. Hot-pressing followed by hot-rolling at 500 °C was adopted. The interfacial microstructure was characterized, the influence of interfacial structure evolution on both mechanical and stamping behavior was explored, and the failure mechanism was analyzed. The results of this study will be conducive to further research on hot-stamping of Ti/Al LMCs.

1 Experiment

1.1 Materials preparation

TA1 pure titanium (Ti) and 2024 aluminum alloy (Al) were selected as raw materials for preparing Ti/Al LMCs. The original thicknesses of Ti and Al are 0.3 and 0.5 mm, respectively, and they were cut to a square with 120 mm in length of side. The preparation process is displayed as Fig.1. Firstly, Ti and Al sheets were ultrasonically cleaned in alcohol for 5 min before drying. Ti and Al were placed alternately along the same direction with Ti as the outermost layer. Then, the prepared 3-, 5- and 7- layers LMCs were placed into a hot-pressing mould. Secondly, hot-pressing was conducted. Ti and Al sheets were stacked and placed in hot-pressing molds and the release agent was sprayed at the same time when the air in
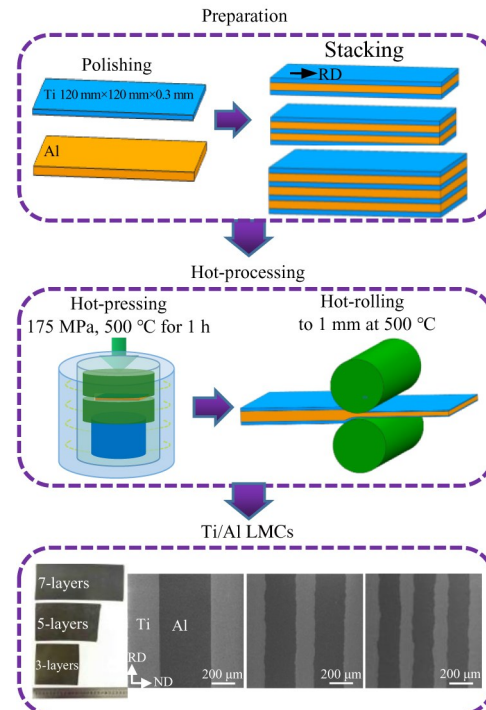

Fig.1   Diagrams of preparing Ti/Al LMCs

the furnace cavity was preheated to about 200 °C. The Ti/Al composites were heated to 500 °C and kept for 20 min, and the pressure of 175 MPa was applied by Y32-315T four-column hydraulic press and kept for 60 min. The Ti/Al LMCs were taken out when the temperature droped to about 200 °C. Thirdly, hot-rolling was conducted at a rotational speed of 20 r/min and the temperature of 500 °C, and LMCs were thinned to 1 mm in thickness. The specific hot-rolling process of LMCs is as follows. The total hot-rolling reduction of 3-layers LMCs was about 8%, and the hot-rolling was completed in one pass. The total hot-rolling reduction of 5-layers LMCs was about 47%, and the hot-rolling was completed in two passes with the reduction of each pass about 25%. The total hot-rolling reduction of 7-layers LMCs was about 63%, and the hot-rolling was completed in three passes; the reduction of the first pass was about 25%, the reduction of the second pass was about 25%, and the reduction of the third pass was about 30%.

1.2 Microstructural examination

Standard mechanical grinding and polishing of metallographic specimens were conducted, and the rolling direction-normal direction (RD-ND) planes were observed. Optical microscope (OM), scanning electron microscope (SEM) and energy dispersive spectrometer (EDS) were used to observe and to analyze the microstructure of each metal layer and interface of LMCs.

1.3 Mechanical performance test

Tensile specimens were cut along RD (0°), 45° and TD (90°) of LMCs, and the gauge dimensions were 6 mm (width) ×25 mm (length). The uniaxial tensile tests were performed by MTS (E45.105) electronic universal testing

machine at room temperature at a speed of 1 mm/min. Three specimens were prepared under each condition. The Vickers microhardness was tested by micro vickers hardness tester (HV-1000) under 0.98 N for 15 s. 7 points were selected for each layer, and the average of the 5 intermediate values was taken as the average microhardness of the layer.

1.4 Stamping formability test

Erichsen cupping test was used to estimate the stamping behavior of LMCs, which was performed by the GBS-60B Erichsen tester equipped with a hemispherical punch with 20± 0.05 mm in diameter, and a speed of 10 mm/min and a clamping force of 10 kN were set. The specimen was cut into a square with 50 mm in length of side. The yield strength ratio (σ_s/σ_b), the work-hardening exponent (n) and plastic strain ratio (r) were adopted to measure the stamping formability of LMCs, and these formability indexes were calculated by mechanical performances.

The work hardening behavior of materials is expressed by Hollomon formula[13–14]:

$$\sigma = k\varepsilon^n \qquad (1)$$

Calculating the natural logarithm on two sides of Eq.(1):

$$\ln\sigma = n\ln\varepsilon + \ln k \qquad (2)$$

The average n ($\bar{n}$) is obtained by the following formula:

$$\bar{n} = (n_0 + 2n_{45} + n_{90})/4 \qquad (3)$$

In Eq.(1−3), k, σ and ε are the hardening coefficient, true stress and true strain, respectively. n_0, n_{45} and n_{90} represent n values in the direction of 0° (RD), 45°, and 90° (TD), respectively. In this study, n is calculated from the slope of the logarithmic curve of the true stress-strain at the stage of uniform plastic deformation.

r represents the strain ratio of LMCs along the plane direction to the thickness direction during uniaxial tension, and its expression is displayed in Eq.(4). The average r ($\bar{r}$) is obtained based on Eq.(5). r_0, r_{45} and r_{90} represent r along 0° (RD), 45° and 90° (TD) of LMCs, respectively.

$$r = \varepsilon_b/\varepsilon_t = \ln(b/b_0)/\ln(L_0b_0/Lb) = -\varepsilon_b/(\varepsilon_b + \varepsilon_L) \qquad (4)$$

$$\bar{r} = (r_0 + 2r_{45} + r_{90})/4 \qquad (5)$$

2 Results and Discussion

2.1 Interfacial microstructure

Fig. 2 displays BSE micrographs of Ti/Al interface. As shown in Fig. 2a, fully dense interfacial bonding without obvious holes or delamination in all LMCs can be observed. During hot deformation, the surface layers of adjacent metals break under high temperature and pressure, and then fresh metals are extruded and bond to achieve a complete mechanical occlusion. However, the Ti/Al interface shows different morphology. As the number of layers increase, Ti/Al
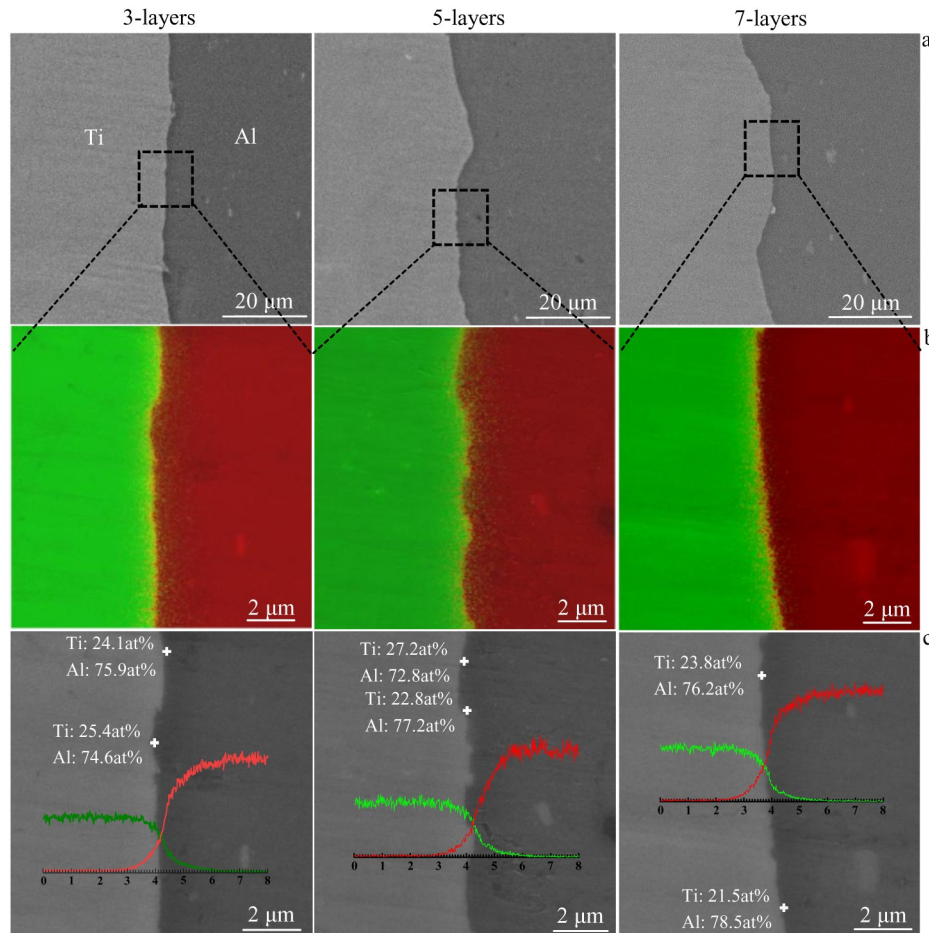

Fig.2　BSE micrographs (a–b) and EDS line scanning results (c) of Ti/Al interface in LMCs

interfaces become rougher. The interface of 3-layers LMCs presents a small wavy shape. The interfacial waviness degree of 5-layers LMCs increases significantly, and obvious prominences and depressions can be seen. The interface of 7-layers LMCs becomes more curved. The rough interface facilitates the adjacent metals to be more firmly embedded into each other, which facilitates interfacial bonding[15]. The rolling reduction of LMCs increases with increasing layers, and the violent coupling of Ti and Al with different deformation resistances during deformation causes the interface become more and more curved. Firstly, Al with fcc lattice can deform on more sliding systems, so the strain distribution is uniform. However, Ti with hcp lattice occupies less independent slip system, which is easy to cause uneven strain distribution. Therefore, Ti and Al possess greatly different deformation resistances, which is easy to produce shear at the interface during deformation. And the larger the deformation, the stronger the shear effect, resulting in more curved interface[16]. Secondly, thermal residual stress is very likely to be induced near the interface during cooling, leading to elastic-plastic deformation. The larger the deformation, the more serious the elastic-plastic deformation, resulting in an increasingly curved interface. The EDS analyses in Fig. 2c show that there is a transition layer at the interface of all LMCs, and the atomic ratio of Ti to Al is approximately 1:3, speculating the formation of $TiAl_3$ phase. The diffusion reaction occurs between Ti and Al during the hot-rolling. Firstly, the solid solutions of Ti (Al) or Al (Ti) are formed, and then $TiAl_3$ crystal nucleus will form at Ti/Al interface when the solid solutions are saturated. The reaction is still going on after the nucleation is completed, and the $TiAl_3$ particles will continue to grow to form a continuous $TiAl_3$ diffusion layer. After that, Ti continuously diffuses into the Al layer, and $TiAl_3$ phase will precipitate from the supersaturated solid solution of Al (Ti) at $TiAl_3$-Al interface when the concentration of Ti exceeds its maximum equilibrium concentration in Al. At the same time, the concentration of Ti in Al layer decreases below the equilibrium concentration, and the concentration of Ti in $TiAl_3$ returns to the equilibrium concentration, which causes Ti atoms to further diffuse into the Al layer. Correspondingly, similar process occurs for Al in Ti layer. The above process is repeated with the prolongation in the reaction time to realize the continuous thickening of $TiAl_3$ phase. $TiAl_3$ phase may be generated during hot deformation at 500 °C[17].

There is an obvious transition zone at Ti/Al interface according to EDS line scanning analysis in Fig. 2c. The width and proportion of the transition zone are shown in Table 1. The widths of transition zone are 2.81, 3.05 and 3.18 μm, and their proportions are 0.400%, 0.731% and 1.053% in 3-layers,

5-layers and 7-layers LMCs, respectively. Therefore, as the layers increase, the width and the proportion of the transition zone increase. The following reasons may need to be considered. First of all, Ti and Al atoms will diffuse across the interface in the process of thermal deformation. As the layers increase, the rougher interface effectively expands to the actual interfacial area, resulting in more intense diffusion[18]. Secondly, dissimilar atomic diffusion occurs through three basic mechanisms: atomic displacement induced by mechanical force, atomic movement along the dislocation channel as well as vacancy diffusion driven by external forces[19]. The rolling reduction increases and their interfacial shearing effect becomes intenser with the increase in layers of LMCs, which introduces plenty of crystal defects, so numerous distortion energy is accumulated. As a result, atom diffusion through the dislocation channel is enhanced. Meanwhile, the conditions such as high temperature and high pressure promote the increase in vacancy concentration near the interface, which strengthens vacancy diffusion. In addition, the thin metal layer is subjected to higher interfacial pressure, which efficiently drives Ti and Al atoms to diffuse more violently[11]. In short, owing to rougher interfacial morphologies, more crystal defects and higher interfacial pressure, 7-layer LMCs exhibit a thicker diffusion zone, which improves the interfacial bonding.

2.2 Mechanical performance

2.2.1 Microhardness

Fig. 3 displays Vickers microhardness distributions of each layer of LMCs. The Vickers microhardness of 1784.188, 1913.156 and 2048.592 MPa of Ti layer, and 703.64, 757.54 and 831.628 MPa of Al layer are measured for 3-layers, 5-layers and 7-layers LMCs, respectively. The Vickers microhardness of both Ti and Al layers increases with increasing the layers of LMCs. LMCs with more layers experience more rolling reduction and introduce more dislocations, which leads to a gradual enhancement in the work hardening effect on both Ti and Al.

The Vickers microhardness of 1281.154, 1359.75 and 1484.7 MPa of Ti/Al interface is measured for 3-layers, 5-layers and 7-layers LMCs, respectively. The increasing microhardness may be explained by the following reasons. Firstly, the interfacial solid solutions and intermetallic phases are beneficial to enhance microhardness. The above EDS analysis has shown that $TiAl_3$ phase is generated, which has extremely high microhardness. As the layers of LMCs increase, the layer of $TiAl_3$ phase thickens, which helps to improve the microhardness of Ti/Al interface. Secondly, as the layers increase, interfacial shearing increases, and the work hardening effect is enhanced due to the introduction of

Table 1   Width and proportion of Ti/Al transition zone in LMCs

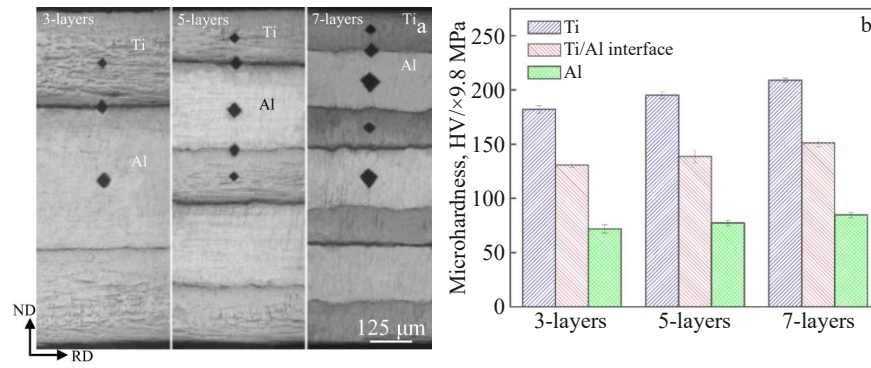| LMCs	Width of transition zone/μm	Width of adjacent Ti and Al/μm	Proportion of transition zone/×10⁻³
3-layers	2.81	702.10	4.00
5-layers	3.05	417.52	7.31
7-layers	3.18	302.03	10.53

Fig.3   Vickers microhardness distributions: (a) micro-indentation and (b) Vickers microhardness value of each layer

plentiful dislocations. Finally, there is a difference in thermal conductivity of Ti and Al, resulting in the generation of thermal stress zones during both thermal deformation and cooling, which introduces thermal mismatch dislocations and also causes high interfacial microhardness.

2.2.2   Tensile performances

Fig. 4 displays the tensile curves, the mechanical performances and the work-hardening rate (θ) curves of LMCs. The mechanical performances including the yield strength (YS), the ultimate tensile strength (UTS), the elongation (EL) and toughness of LMCs are calculated in Table 2. It is noted that both YS and UTS in all LMCs decrease along RD, TD and 45° in turn, which shows obvious anisotropy resulting from the strong basal texture formed in component metals during hot-rolling. The average YS of 283.10, 288.33, 294.48 MPa, and the average UTS of 354.70,

360.70, 366.68 MPa are obtained for 3-layers, 5-layers and 7-layers LMCs, respectively. Both the average YS and UTS of LMCs are enhanced with increasing the layers. EL and toughness in all LMCs decrease along RD, 45° and TD in turn. The average EL of 17.71%, 15.65%, 13.96%, and the average toughness of 60.61, 53.36, 49.07 J·m^{-3} are obtained for 3-layers, 5-layers and 7-layers LMCs, respectively. Both average EL and average toughness decrease with increasing the layers. The rolling reduction of LMCs increases and more dislocations are introduced with the increase in layers. Usually, materials with more dislocations possess inferior ductility, which is attributed to strain localization resulting from lower strain hardenability[20]. As the strain increases, the θ in all LMCs is continuously reduced, as shown in Fig. 4e, indicating that the main deformation mechanism of LMCs is dislocation slip[21]. Compared with other LMCs, the decrease
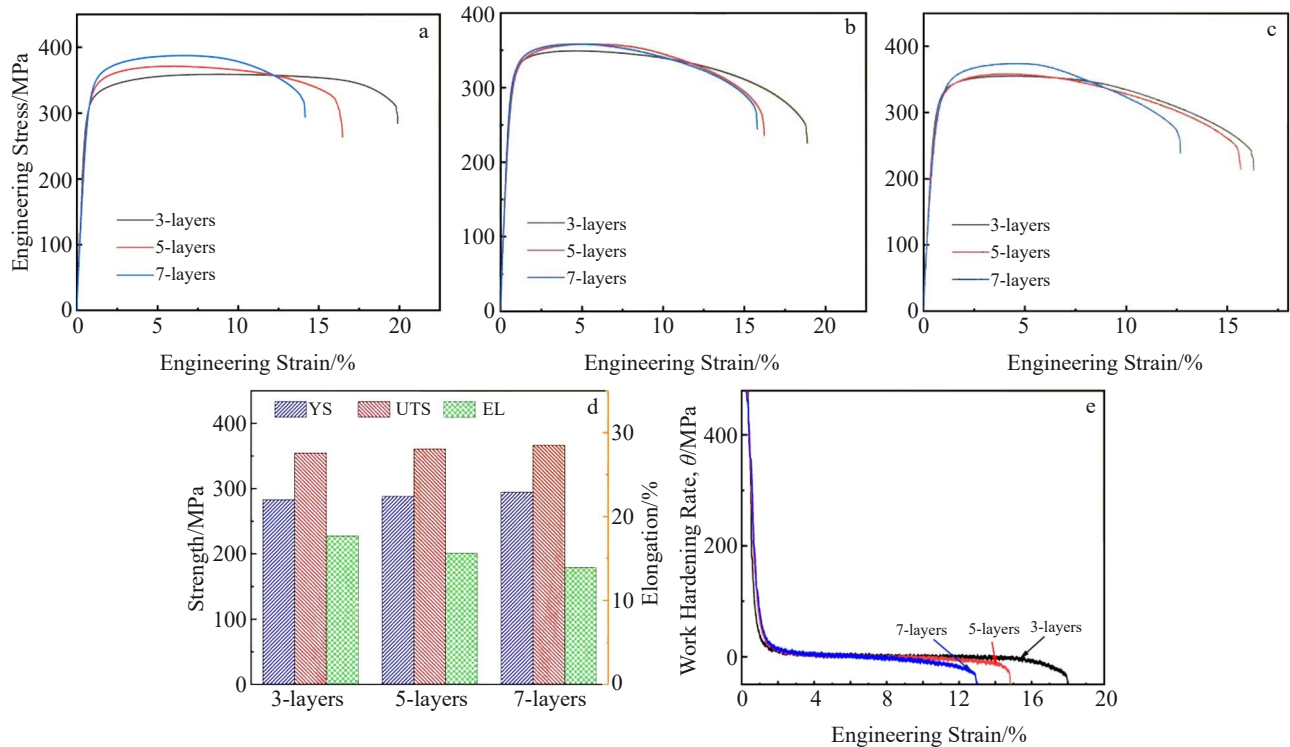

Fig.4   Tensile curves of LMCs in RD (a), 45° (b) and TD (c); mechanical performances (d); work hardening rate (θ) curves (e)

Table 2   Mechanical performances including YS, UTS, EL and toughness of LMCs in different directions

LMCs	Direction	YS/MPa	$\overline{YS}$/MPa	IPA/%	UTS/MPa	$\overline{UTS}$/MPa	IPA/%	EL/%	$\overline{EL}$/%	IPA/%	Toughness/J·m⁻³	Average toughness/J·m⁻³
	RD	296.81±1.19			366.12±3.39			18.40±0.72			68.54±4.03	
3-layers	45°	273.25±3.14	283.10	6.93	335.59±1.99	354.70	4.68	18.16±1.97	17.71	5.60	60.83±3.86	60.61
	TD	279.25±4.15			362.38±3.37			16.58±3.45			52.46±2.76	
	RD	308.87±4.81			376.53±1.68			16.75±0.30			57.60±2.57	
5-layers	45°	274.64±0.04	288.33	9.97	340.87±1.01	360.70	6.31	15.40±4.70	15.65	9.85	52.16±5.53	53.36
	TD	281.48±1.43			364.69±0.26			14.80±0.18			50.30±3.30	
	RD	317.77±0.78			390.92±2.74			15.22±1.32			51.17±4.64	
7-layers	45°	279.12±2.24	294.48	10.99	343.81±2.93	366.68	9.30	14.11±0.93	13.96	12.37	53.49±6.97	49.07
	TD	286.56±7.25			365.31±0.88			12.56±1.43			42.55±3.38	

rate of θ of 3-layers LMCs is the fastest during the elastic-plastic stage, while the θ decreases less during the following uniform plastic deformation, and higher θ retention rate is presented, which is the key for its high ductility. Finally, the materials break under high strain. The decrease rate of θ, θ retention rate and fracture strain of 5-layers and 7-layers LMCs decrease successively.

The in-plane anisotropy (IPA) index is adopted to characterize the anisotropy of mechanical performances of sheets[22]:

$$IPA = \frac{2P_{max} - P_{mid} - P_{min}}{2P_{max}} \qquad (6)$$

where P_{max}, P_{mid} and P_{min} express the largest, median and the smallest mechanical parameters including UTS, YS and EL along different directions, respectively. IPA of YS is 6.93%, 9.97% and 10.99%, IPA of UTS is 4.68%, 6.31% and 9.30%, and IPA of EL is 5.60%, 9.85% and 12.37% in 3-layers, 5-layers and 7-layers LMCs, respectively. The above data show

that the mechanical performances of LMCs are obviously anisotropic, and the anisotropy becomes more obvious for LMCs with more layers.

SEM micrographs of the fracture surface of LMCs are shown in Fig. 5. LMCs are subjected to violent plastic deformation, and the characteristics of delamination and necking are observed at the fracture. Interfacial debonding plays a crucial role during the fracture of LMCs. On the one hand, constraint strain is easily introduced into the interface owing to the discordant deformation of Ti and Al, which may induce interface debonding. On the other hand, intense stress concentration is generated near Ti/Al interface owing to the discrepant necking degrees of Ti and Al. Thus, interfacial debonding will be obviously observed. Moreover, interfacial debonding may be induced by the brittle TiAl₃[23]. The deformation of LMCs increases with increasing the layers, which promotes the improvement of interfacial bonding according to the film theory. The degree of interfacial debonding decreases, and the
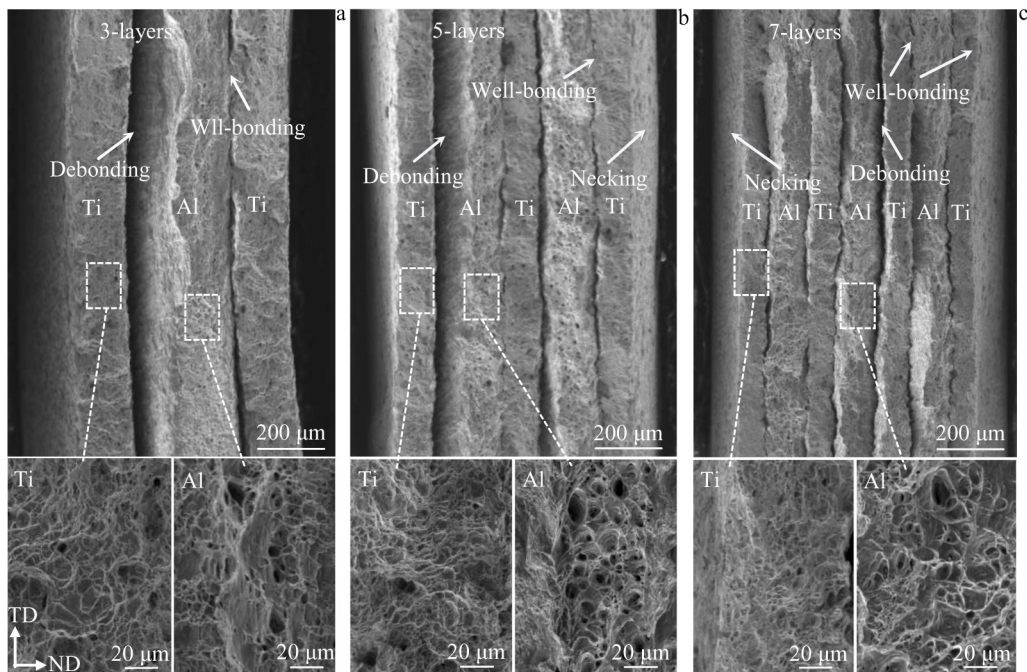

Fig.5   SEM micrographs of the fracture surface of LMCs with 3-layers (a), 5-layers (b) and 7-layers (c)

area with well-bonding increases significantly with increasing the layers of LMCs. Both Ti and Al show ductile rupture features. Many small and uniform dimples are distributed, and severe necking can be easily seen in Ti layer of 3-layers LMCs, indicating excellent ductility. There are plentiful tearing traces and non-uniform dimples in Ti layer with increasing the layers of LMCs, which is due to the local plastic instability in Ti matrix caused by large deformation. Al layer is distributed in a dimple shape with a conical appearance, and severe tearing traces and non-uniform dimples can be observed in Al layer of 3-layers LMCs. The dimples grow and deepen with increasing the layers of LMCs. These characteristics show that the ductility of both Ti and Al layers is deteriorated for LMCs with more layers.

2.3 Room-temperature stamping formability

2.3.1 Formability indexes

σ_s/σ_b, n and r greatly affect the stamping behavior of LMCs, as shown in Table 3. The average σ_s/σ_b ($\overline{\sigma_s/\sigma_b}$) of 0.7985, 0.7993 and 0.8031 are obtained for 3-layers, 5-layers and 7-layers LMCs, respectively. $\overline{\sigma_s/\sigma_b}$ is enhanced gradually with increasing the layers of LMCs. Materials with low σ_s/σ_b can effectively avoid early instability deformation and necking of sheet, resulting in high ductility and facilitating its forming[20]. Pan et al[24] found that strong basic texture will lead to high yield strength, namely relatively large σ_s/σ_b, which will further reduce the formability of the sheet. For LMCs with fewer layers, the lower $\overline{\sigma_s/\sigma_b}$ represents that they undergo a relatively long uniform plastic deformation, which is conducive to enhance its local strain capacity. Both small σ_s/σ_b and high EL contribute to the formability enhancement of LMCs.

The calculation of n is listed in Fig. 6. $\bar{n}$ of 0.0663, 0.0638 and 0.0609 are obtained for 3-layers, 5-layers and 7-layers LMCs, respectively. $\bar{n}$ is gradually reduced with increasing the layers of LMCs. Chanda et al[25] found that pure aluminum cold-rolled by 75% has lower n than that cold-rolled by 50%. A higher n will weaken or even avoid plastic instability, thereby improving the formability[26]. Previous studies have reported that sheets with weaker basal texture have a larger n[27]. Many grains will choose a favorable orientation to deform, and the orientation softening effect is significant, which can maintain a more durable deformation and result in a greater limiting forming capacity. Especially, some researchers have
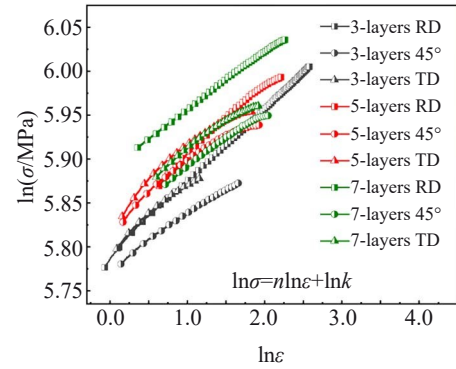

Fig.6 Logarithmic curves of true stress-strain at the stage of uniform plastic deformation of LMCs

showed that a higher n value of sheet may be related to its lower yield strength and higher EL[28]. The aforesaid results correspond to the conclusions displayed in Table 2.

Tensile specimens with a true strain of 9% are measured to calculate r. $\bar{r}$ of 1.66, 1.54 and 1.42 are obtained for 3-layers, 5-layers and 7-layers LMCs, respectively. $\bar{r}$ of LMCs is gradually reduced with increasing the layers. As the layers increase, the quantity of interface increases, and the stress-strain transferring via the interface is conducive to alleviate strain localization. Therefore, LMCs along the plane direction and thickness direction have well coordinated deformations, causing a reduction in r. LMCs with a large r have a strong resistance to thinning, and it can be inferred that they will get larger ultimate cup depth in Erichsen cupping test.

2.3.2 Stamping formability

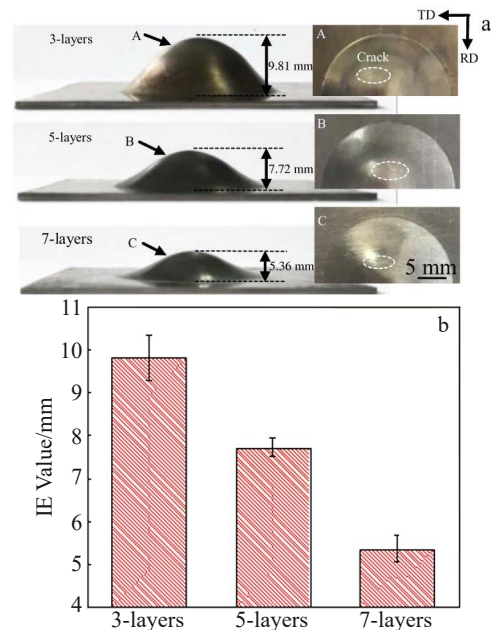Fig.7 shows the Erichsen cupping tests and the IE values of LMCs. The IE values of 9.81, 7.72 and 5.36 mm are obtained

Table 3 σ_s/σ_b, n and r of LMCs in RD, 45° and TD

LMCs	Direction	σ_s/σ_b	$\overline{\sigma_s/\sigma_b}$	n	$\bar{n}$	r	$\bar{r}$
	RD	0.8107		0.0824		1.28	
3-layers	45°	0.8142	0.7985	0.0570	0.0663	1.79	1.66
	TD	0.7706		0.0686		1.79	
	RD	0.8203		0.0764		1.71	
5-layers	45°	0.8057	0.7993	0.0577	0.0638	1.62	1.54
	TD	0.7772		0.0632		1.21	
	RD	0.8129		0.0651		1.20	
7-layers	45°	0.8188	0.8031	0.0598	0.0609	1.41	1.42
	TD	0.7844		0.0591		1.66	

Fig.7 Chematic of Erichsen cupping tests (a) and IE values (b) of LMCs

for 3-layers, 5-layers and 7-layers LMCs, respectively. 3-layers LMCs possess the most excellent formability. The IE value gradually decreases with increasing the layers of LMCs, and the poor formability is consistent with the low ductility obtained by the tensile test[29]. The rolling deformation increases with increasing the layers, producing plentiful dislocations in LMCs. Therefore, the local flow resistance of LMCs with more layers under biaxial stress is greatly increased due to the strong work hardening effect, which is easy to reach the ultimate strength of LMCs, and thus break accurs, resulting in poor formability. The formability of LMCs is also greatly affected by the texture. The larger the rolling deformation, the stronger the rolling texture, and the stronger the texture to deteriorate the formability[30]. According to the formability indexes displayed in Table 3, as the layers of LMCs increase, the gradually increasing σ_s/σ_b indicates that the uniform plastic deformation stage of LMCs is relative short and the local strain capacity is weaker, which is not conducive to forming. $\bar{n}$ is gradually reduced with increasing the layers, and LMCs are prone to strain localization, which leads to the partial thinning of cup forming specimens and easy cracking. $\bar{r}$ decreases with increasing the layers, which indicates that the ability of LMCs to resist thinning decreases and their forming limit is reduced. The formability indexes

correspond to the conclusions of the formability of LMCs strictly. It can be seen from the locally enlarged images of region A, B and C in Fig.7a that all cup specimens experience the greatest strain at some locations to the dome, and the crack direction in all cup forming specimens is almost along TD.

The stress-strain distribution in Ti and Al layers during cup drawing forming is greatly affected by the interfaces. For the purposes of revealing their stress-strain state, Vickers microhardness at different positions and thicknesses of different layers for cup forming specimens are measured, as displayed in Fig. 8. Firstly, the microhardness of Ti, Ti/Al interface and Al is tested at three areas of the bottom, dome and crack, as displayed in the bar charts of Fig.8. Although the bottom of cup forming specimens sustains the blank holding force, the force is relatively dispersed, and the resulting strain is very small, so the Vickers microhardness is close to that of the original sheet. The crack area suffers from the highest strain, and the strain hardening effect is the strongest, which possesses the highest Vickers microhardness, followed by the dome. Hence, the Vickers microhardness of cup forming specimens decreases in the order of crack area, dome and bottom. It is noted that the Vickers microhardness of each layer increases with increasing the layers, which reflects the strengthening of strain hardening effect. The thicknesses of
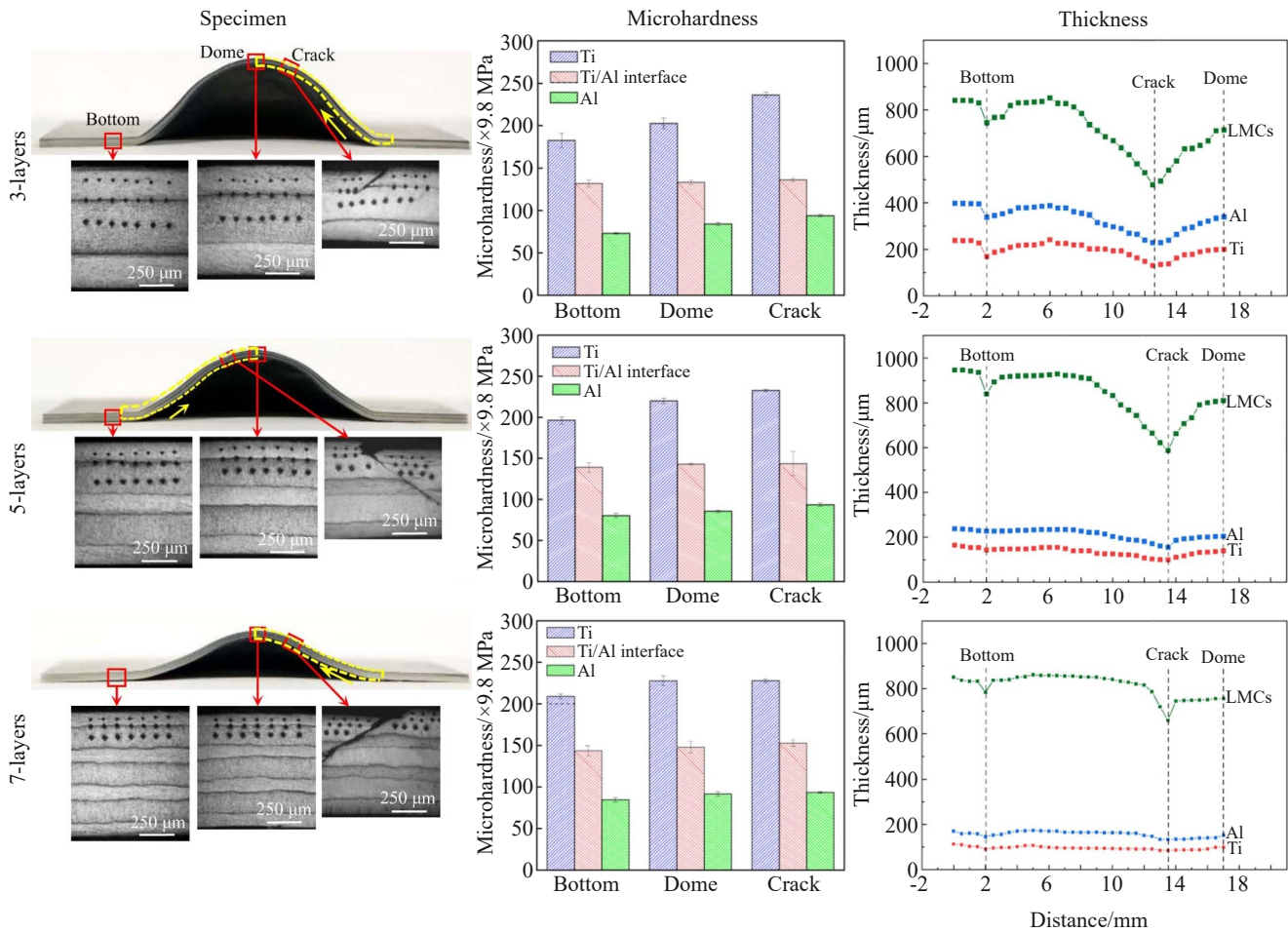

Fig.8   Microhardness and the thickness evolution of cup forming specimens of LMCs

Table 4   Thickness reduction of cup forming specimens at the crack and dome (%)

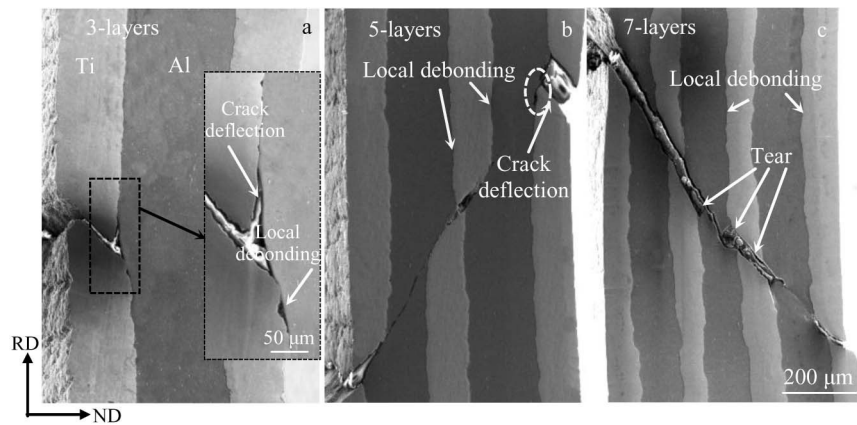| LMCs	Reduction of LMCs		Reduction of Ti		Reduction of Al	
	Crack	Dome	Crack	Dome	Crack	Dome
3-layers	43.17	15.14	45.29	16.20	42.50	14.49
5-layers	38.00	14.45	40.03	15.64	34.82	14.01
7-layers	22.35	11.05	24.49	12.42	21.72	10.90

Fig.9   Fracture characteristics of cup forming specimens: (a) 3-layers, (b) 5-layers, and (c) 7-layers

LMCs, Ti and Al layers at intervals of 0.5 mm from the bottom to dome of cup forming specimens are displayed in Fig. 8. It can be found that the thinning of the crack is the greatest, followed by the dome, and their thickness changes are listed in Table 4. Compared to Al, the thickness thinning of Ti is more serious at both the crack and the dome. Ti is not easy to deform due to higher YS, but Ti possesses a higher Poisson ratio, so its deformation along TD is greater[12]. The thickness thinning of LMCs, Ti and Al decreases with increasing the layers. And the least thickness reduction occurs in 7-layers LMCs, indicating that the ultimate deformation capacity of 7-layers LMCs is low due to the adverse influence of work hardening, so its formability is poor.

Fig. 9 presents the fracture characteristics of cup forming specimens. The outer Ti layer of 3-layers LMCs undergoes the most severe deformation, causing the crack to start and to spread rapidly to the interface. Then, the crack deflects at the location of interfacial debonding due to the weak interfacial bonding. The interface is prone to local debonding in the process of cup forming, and then the locations of local debonding will be connected to each other when the stress is large enough, resulting in interfacial delamination. Interfacial delamination is the dominant fracture mechanism. Due to crack deflection and blunting at the interface, the energy of crack growth is partially released, which prevents crack growth to some extent, and crack re-nucleation requires more energy[31]. Therefore, 3-layers LMCs show excellent formability. Previous studies have also confirmed that interfacial delamination can improve the toughness of LMCs by inhibiting crack initiation, promoting crack deflection and reducing the driving force of crack growth[32]. As the layers of LMCs increase, their interfacial bonding strength is improved, severe interfacial delamination does not occur, and only slight local debonding occurs at the fracture. The cracks start in the outer Ti layer, then slightly deflect and tear as they extend to the interface, and finally rapidly penetrate the entire LMCs. Due to more interfaces and good interfacial bonding, the cracks grow rapidly, and eventually fracture failure of LMCs occurs quickly, which deteriorates the formability.

3 Conclusions

1) Ti/Al LMCs with 3, 5 and 7 layers are prepared by hot-pressing followed by hot-rolling at 500 °C. The influence of interface constraint on the mechanical performance and stamping formability of LMC is studied, and the crack initiation and growth mechanisms are discussed.

2) All LMCs are fully dense and exhibit good interfacial bonding. As the layers increase, the Ti/Al interface becomes rougher, the $TiAl_3$ phase layer thickens gradually, and the interfacial microhardness increases gradually.

3) YS and UTS increase accompanied with the reducing in EL and toughness, and the anisotropy of mechanical performances increases with increasing the layers of LMCs. High density dislocation is introduced in LMCs during hot-rolling, resulting in enhanced strain strengthening effect. Also, the $TiAl_3$ phase with high strength contributes to the increase in strength of LMCs. Meanwhile, materials with more dislocations possess poor ductility and toughness, which is attributed to strain localization resulting from lower strain hardenability. Strong basal texture is formed during rolling, which makes LMCs show obvious anisotropy.

4) The stamping formability is reduced with increasing the layers of LMCs. Both the increased σ_s/σ_b and decreased n, r deteriorate the stamping formability of LMCs. The interface of 3-layers LMCs is easy to debonding, which makes LMCs show excellent stamping formability by inhibiting crack

initiation, promoting crack deflection and passivation and reducing the driving force of crack growth. The interfacial bonding becomes stronger for LMCs with more layers, and the cracks deflect and tear slightly as they grow to the interface. The crack growth is rapid due to more interfaces and good interfacial bonding, and then LMCs break quickly, which deteriorates their formability.

References

1 Qiang Meng, Yang Xirong, Liu Xiaoyan *et al. Rare Metal Materials and Engineering*[J], 2023, 52(5): 1673

2 Zhang Wanpeng, Lang Lihui, Zang Bo *et al. Rare Metal Materials and Engineering*[J], 2023, 52(6): 2085 (in Chinese)

3 Li Yan, Liu Qi, Li Jucai *et al. Rare Metal Materials and Engineering*[J], 2023, 52(6): 2017

4 Wu Xiaoming, Shi Changgen, Fang Zhonghang *et al. Rare Metal Materials and Engineering*[J], 2022, 51(1): 286 (in Chinese)

5 Cao Miao, Wang Cuiju, Deng Kunkun *et al. Journal of Materials Research and Technology*[J], 2021,14: 1655

6 Li Boxin, Niu Jiale, Feng Zhibin *et al. Rare Metal Materials and Engineering*[J], 2023, 52(6): 2010

7 Zhang Gaowei, Han Wentuo, Zhang Lei *et al. Rare Metal Materials and Engineering*[J], 2022, 51(10): 3943 (in Chinese)

8 Zhao Tianli, Bing Zhang, Zhang Zhijuan *et al. Rare Metal Materials and Engineering*[J], 2022, 51(10): 3663

9 Lee S B, Ledonne J E, Lim S C V *et al. Acta Materialia*[J], 2012, 60(4): 1747

10 Zhang Xuanchang, Wang Cuiju, Deng Kunkun *et al. Materials Science and Engineering A*[J], 2019, 761: 1

11 Fan Minyu, Domblesky Joseph, Jin Kai *et al. Materials & Design*[J], 2016, 99: 535

12 Kaya İrfan, Ömer Necati Cora, Doğan Acar *et al. Metallurgical and Materials Transactions A*[J], 2018, 49(10): 5051

13 Liu Baoxi, Zhang Shijian, Lin Fuxing *et al. Materials China*[J], 2024, 43(1): 35 (in Chinese)

14 Del Valle J A, Ruano O A. *Scripta Materialia*[J], 2006, 55(9): 775

15 Xing Binghui, Huang Tao, Song Kexing *et al. Vacuum*[J], 2023, 210: 1

16 Mo Taiqian, Liu Siyuan, Yang Rongchao *et al. Materials Characterization*[J], 2023, 202: 1

17 Zhang Jianyu, Wang Yanhui, Lü Zheng *et al. Transactions of Nonferrous Metals Society of China*[J], 2022, 32(2): 524

18 Mo Taiqian, Xiao Huaqiang, Lin Bo *et al. Journal of Materials Research and Technology*[J], 2022, 19: 520

19 Cao Miao, Wang Cuiju, Deng Kunkun *et al. Materials Research*[J], 2020, 23(1): 1

20 Fitsum Feyissa, Ravi Kumar D, Nageswara Rao P. *Journal of Materials Engineering and Performance*[J], 2018, 27(4): 1614

21 Chen Wenhuan, He Weijun, Chen Zejun *et al. International Journal of Plasticity*[J], 2020, 133: 1

22 Singh R K, Singh A K, Prasad N E. *Materials Science and Engineering A*[J], 2000, 277(1–2): 114

23 Zhang Xiaobo, Yu Yangbo, Liu Bin *et al. Journal of Alloys and Compounds*[J], 2019, 783: 55

24 Pan Fusheng, Wang Qinghang, Jiang Bin *et al. Materials Science and Engineering A*[J], 2016, 655: 339

25 Chandra S K, Narayanasamy R. *Materials Today: Proceedings*[J], 2018, 5(2): 6888

26 Wang Lifei, Zhang Zhengyong, Cao Miao *et al. JOM*[J], 2019, 71(5): 1705

27 Ying Yang, Guo Dizi, Du Yan *et al. Titanium Industry Progress*[J], 2022, 39(6): 1 (in Chinese)

28 Wang Lifei, Pan Xiaohuan, Zhu Xingxiao *et al. Transactions of Nonferrous Metals Society of China*[J], 2023, 33(4): 1066

29 Wang L, Strangwood M, Balint D *et al. Materials Science and Engineering A*[J], 2011, 528(6): 2648

30 Hong Quan, Guo Ping, Zhou Wei *et al. Titanium Industry Progress*[J], 2022, 39(5): 27 (in Chinese)

31 Wang Honglin, Ma Jian, Yuan Meini *et al. Materials Today Communications*[J], 2022, 33: 1

32 Chatdanai B, Angkrich T. *Composite Structures*[J], 2019, 229: 1

界面约束作用下 Ti/Al 多层复合材料的力学性能和冲压成形性能

曹　苗[1]，邓坤坤[2]，陈慧琴[1]，段兴旺[1]，徐　月[1]，李　飞[1]，车　鑫[1]，王振博[1]，杨景然[1]，张志豪[1]，李　烨[1]
(1. 太原科技大学 材料科学与工程学院，山西 太原 030024)
(2. 太原理工大学 材料科学与工程学院，山西 太原 030600)

摘　要：采用热压+热轧复合法在 500 ℃制备了 3 层、5 层和 7 层配置的 Ti/Al 多层复合材料（LMCs），研究了拉伸和埃里克森杯突试验过程中复合板的裂纹萌生和扩展行为，分析了界面约束效应对复合板力学性能和冲压成形性能的影响机理。结果表明，复合板界面具有微米级厚度的金属间相，导致其具有较强的界面结合。随复合板层数的增加，其屈服强度（YS）和极限抗拉强度（UTS）增加，延伸率（EL）和韧性降低，且由于热轧形成了强基面织构，复合板力学性能的各向异性明显增加。同时，复合板的加工硬化指数（n）和塑性应变比（r）均降低，屈强比（σ_s/σ_b）增大，这些均导致了复合板的冲压成形性能变差。对于层数较少的复合板，在断裂过程中界面脱粘起了主要作用。由于界面结合不佳，界面易发生分层，通过抑制裂纹萌生、促进裂纹偏转和钝化、降低裂纹扩展的驱动力，有效地延缓了复合板的断裂失效。
关键词：Ti/Al 多层复合材料；拉伸；埃里克森杯突试验；界面

作者简介：曹　苗，女，1991 年生，博士，讲师，太原科技大学材料科学与工程学院，山西 太原 030024，E-mail：2022009@tyust.edu.cn